energies

Article

An Experimental Analysis and ANN Based Parameter Optimization of the Influence of Microalgae Spirulina Blends on CI Engine Attributes

S. Charan Kumar [1], Amit Kumar Thakur [1], J. Ronald Aseer [2], Sendhil Kumar Natarajan [2], Rajesh Singh [3], Neeraj Priyadarshi [4] and Bhekisipho Twala [5,*]

1 Department of Mechanical Engineering, Lovely Professional University, Punjab 144401, India
2 Department of Mechanical Engineering, National Institute of Technology Puducherry, Karaikal 609609, India
3 Uttaranchal Institute of Technology, Uttaranchal University, Dehradun 248012, India
4 Department of Electrical Engineering, JIS College of Engineering, Kolkata 741235, India
5 Digital Transformation Portfolio, Tshwane University of Technology, Staatsartillerie Rd., Pretoria West, Pretoria 0183, South Africa
* Correspondence: twalab@tut.ac.za

Abstract: In this present investigation, emittance and performance attributes of a diesel engine using micro-algae spirulina blended biodiesel mixtures of various concentrations (20%, 35%, 50%, 65%, 80%, and 100%) were evaluated. An optimization model was also developed using an Artificial Neural Network (ANN) to characterize the experimental parameters. Experimental findings demonstrated significant improvement in brake specific fuel consumption (BSFC) using varied blends. Furthermore, brake thermal efficiency (BTE) is decreased gradually for biodiesel blends as compared to diesel. Micro-algae spirulina blends have shown lower concentrations of NO_X and HC while increasing CO_2 relative to pure diesel. To develop the model, three sets of optimizers, namely, adam, nadam, and adagrad, along with activation functions, such as sigmoid, softmax, and relu, were selected. The results revealed that sigmoid activation function with adam learning optimizer by using 32 hidden layer neurons has given the least value of mean squared error (MSE). Hence, the ANN approach was proven to be capable of predicting engine attributes with a least mean squared error of 0.00013, 0.00060, 0.00021, 0.00011, and 0.00104 for NO_X, HC, CO_2, brake thermal efficiency, and brake specific fuel consumption, respectively. The Artificial Neural Network approach is capable of predicting CI engine attributes with accuracy and ease of investigation.

Keywords: Artificial Neural Network; biofuels; CI engine; micro-algae spirulina

check for updates

Citation: Kumar, S.C.; Thakur, A.K.; Aseer, J.R.; Natarajan, S.K.; Singh, R.; Priyadarshi, N.; Twala, B. An Experimental Analysis and ANN Based Parameter Optimization of the Influence of Microalgae Spirulina Blends on CI Engine Attributes. *Energies* **2022**, *15*, 6158. https://doi.org/10.3390/en15176158

Academic Editor: Maria Founti

Received: 27 July 2022
Accepted: 22 August 2022
Published: 24 August 2022

Publisher's Note: MDPI stays neutral with regard to jurisdictional claims in published maps and institutional affiliations.

Copyright: © 2022 by the authors. Licensee MDPI, Basel, Switzerland. This article is an open access article distributed under the terms and conditions of the Creative Commons Attribution (CC BY) license (https://creativecommons.org/licenses/by/4.0/).

1. Introduction

Diesel engines are the predominant source of power generation that are extensively employed in automotive, defense, maritime, mining, etc., industries due to their superior fuel efficiency and sturdy character. Considering our currently existing stockpiles of fossil fuels and the increasing pace of their use, they will be completely depleted. As a result, the breadth and potential of alternative energy sources are substantial. Bio-fuels [1–3] are gaining popularity around the world as a viable adjunct to standard fuel. Even though biofuels have lower efficiency as opposed to diesel, they are widely favored due to reduced emissions. Bio-fuels can indeed be utilized in engines by mingling them with diesel in a particular ratio without requiring substantial alterations in engine hardware. Its fuel rating and thermo-physical attributes are akin to diesel with high oxygen (O_2) concentration [4]. Bio-fuels extracted from micro and macro-algae [5], non-edible [6], and edible [7] feedstocks are regarded as third, second, and first-generation biofuels, respectively. Regardless of the requirement for empirical investigation, to gain a comprehensive insight into engine characteristics when utilizing bio-fuels, lately, there's been an upsurge in employing various methodologies to simulate engine behavior. These approaches reduce expense and processing time, alongside minimizing the dependency on the requirement for empirical investigation [8,9]. ANN [10] is one such approach. ANN is regarded as a cost-effective [11] and efficient solution for resolving a broad range of automotive challenges [12,13].

Alcohol-bio-diesel combinations were utilized to evaluate diesel engine attributes. Datta et al. [14] observed that for the alcohol-bio-diesel mixture, NO_X reduced and enhanced efficiency. NO_X was reported to be significantly higher in a TCCI engine powered using an alternative fuel derived from soybean and castor oil; however, soybean emitted more NO_X as opposed to castor oil [15]. Chlorella protothecoides were examined, and recommendations for identifying Chlorella protothecoides as feasible fuel resources for CI engines were indeed considered [16]. Pongamia piñata-based bio-diesel has been reported to have improved HC and CO concentrations than canola bio-diesel [17,18]. A premixed charged CI-DI engine utilizing cottonseed bio-diesel generated enhanced BTE, and emissions such as NO_X, CO, and HC were slightly reduced [19]. The CI engine attributes running on the B20 combination of Thumba bio-diesel were investigated. When opposed to baseline fuel (diesel), B20 blends had shown improved performance in terms of BTE, but NO_X elevated [20]. Satputaley et al. [21] tested the influence of Chlorella Protothecoides (CP100) bio-diesel on the CI engine. When contrasted to conventional fuel, the CP100 significantly decreases CO by 4.2%, EGT by 6.1%, and brake power by 7.0%. It was apparent that bio-fuel derived using micro-algae increases BSFC whilst reducing emissions [22]. For reducing the number of expenditures, search time, and experimental trials non-linear and linear algorithms, namely, RSM, factorial design, ANN, and genetic algorithms, are utilized to assess engine behavior [23]. In comparison to the RSM model, ANN has the most reliable estimations and a high correlation between observed and predicted outcomes, making it an excellent learning strategy [24]. A significant advancement in the numerical evaluation of CI engine attributes is advanced modeling using ANN [25]. The results obtained for Ricinuscommunis seed bio-diesel were anticipated using an ANN framework [26]. Orange peel oil-diesel blends were explored as an alternative to conventional diesel in CI engines [27]. For blend proportion of 70% diesel and 30% orange peel oil, BSEC decreased by 19%, and BTE enhanced by 16.5% at peak load. By using the Quasi–Newton algorithm, an ANN model was developed. The R^2 values are 0.986 and 0.994 for BSEC and BTE, respectively, for the ANN model. The viability of Karanja oil as a biodiesel feedstock was examined [28]. Test fuel concentrations composed of 50%, 40%, 30%, 20%, 10%, and 0% by volume. Findings demonstrated that as the proportion of biodiesel enhances, so does the BSFC. Furthermore, with a rise in blend concentration HC and CO drops considerably. Numerical validation was carried out by Neurosolution software. Five sets of inputs were selected for network training. They concluded that the test and model outcomes were highly correlated. The correlation coefficient was in the acceptable range of 0.98–0.99 for all parameters. As demonstrated by Bahri et al. [29], the ANN model can indeed be applied as a real technique for engine operations, which predicted combustion noise levels considerably lower than 0.5 percent deviation. The efficacy of honing oil-derived bio-diesel was explored by Channapattana et al. [30] at varying percentages (20 to 100) in a CI-DI engine. They performed ANN simulation to evaluate the experimental outcomes. Thermal efficiency, carbon monoxide, exhaust gas temperature, hydrocarbons, specific fuel consumption, nitrogen oxide, and smoke were used as output elements. Algorithms trainscg, traingdx, trainrp, and trainlm were used to update the parameters (training). They observed that 28 neurons in the hidden layer yield the highest r and least mean squared error for the trainlm algorithm.

There is exhaustive information available on the attributes (emissions and performance) of bio-fuel fueled CI engines from the second and first-generation feed-stock. The current research arose from several prior investigations that revealed a lack of research on spirulina micro-algae bio-diesel (third generation). Furthermore, the design and implementation of the ANN are currently limited for evaluating engine characteristics, necessitating additional research. This investigation is split into two phases. Firstly, this study explores the impact of spirulina bio-diesel amalgams of SB100, SB80, SB65, SB50, SB35, SB20, and

SB0 on emissions (NO_X, UHC, and CO_2) and performance (BTE and BSFC) attributes of the CI engine (explained in Sections 2 and 4). Secondly, to build an ANN model able to accurately forecast the behavior of a CI engine (explained in Sections 3 and 4). The code for ANN was written in Python with Keras framework and Tensor flow as back-end. The impact of ANN factors such as training algorithm, types of the transfer function, epochs, and the number of neurons on the accuracy of the prediction of the model is assessed.

2. Materials and Methods

Fuel Properties and Test Rig

In this investigation, diesel and bio-diesel derived from spirulina micro-algae were used and were evaluated as a CI engine fuel substitution, which was obtained from Planet Industries Pvt Ltd., New Delhi, India. For assessing the fuel attributes (kinematic viscosity, flash point, calorific value, and density), diesel fuel (SB0: 100% diesel) was employed as a baseline. SB100 (100% spirulina), SB80 (80% spirulina + 20% diesel), SB65 (65% spirulina + 35% diesel), SB50 (50% spirulina + 50% diesel), SB35 (35% spirulina + 65% diesel), SB20 (20% spirulina + 80% diesel), and SB0 (100% diesel) are taken at volume basis as test fuels. The attributes (physico-chemical) of the fuel selected in this analysis are presented in Table 1. The evaluated fuel attributes were tested as per ASTM (American Society for Testing and Materials) standards and proven to be a viable replacement for use in diesel engines.

Table 1. Physico-chemical attributes of test fuels.

Test Fuel	Density (kg/m^3) at 15 °C	Flash Point (°C)	Calorific Value (MJ/kg)	Viscosity (mm^2/s)
Spirulina (SB100)	860	130	41	5.22
SB 80	854.8	118.3	41.29	4.63
SB 65	849.1	108.5	41.46	4.37
SB 50	843.4	100.7	41.63	3.92
SB 35	840.9	95.3	41.97	3.56
SB 20	835.7	86.5	42.6	3.19
Diesel (SB0)	830	70	43	3

The analysis was conducted on a CI 4-stroke, water-cooled 1-cylinder engine, to evaluate how spirulina bio-diesel blends impact the emissions and performance attributes. Table 2 summarizes the technical specifications of the experimental engine employed. The experimental engine is depicted in schematic form in Figure 1. Throughout the experiment, injection timing and injection pressure were held constant. The load on the engine varied from 0 to 10 kg keeping the speed of the engine at a constant value at 1500 rpm. The test rig incorporated a multi-gas analyzer (MN-05, manufactured by Mars Technologies, for measuring emissions), fuel control valve, fuel tank (bio-diesel and diesel), eddy current dynamometer, air filter, air box, and rotameter. Throughout the process of the experimentation:

- The engine's fuel system, cooling, and lubrication have all been inspected for proper operation;
- To achieve steady operating circumstances, the engine is started and operated in no-load for 25 min using baseline fuel (diesel);
- Data were taken within a few minutes of attaining steady operating circumstances;
- All relevant data were carefully obtained manually. The tests were executed for varied loads (0, 2, 4, 6, 8, and 10 kg) using SB100, SB80, SB65, SB50, SB35, SB20, and SB0 fuels, emissions, and performance attributes were written down;
- NO_X, and HC were recorded in ppm whereas CO_2 was in percentages;
- Each experiment was undertaken three times, and the mean value was noted. Table 3 shows the uncertainty measurements of the obtained outcomes.

Table 2. Test rig technical specifications.

Engine Specifications	
Maker	Kirloskar, TV1
Indicator used type	Cylinder pressure
Dynamometer type	Eddy current
Cooling type	Water
Number of Cylinders	One
Compression ratio	17.5
Stroke type	Four
Connecting rod length	234 mm
Engine power	5.2 kW
Cylinder bore	87.5 mm
Stroke length	110 mm
Maximum speed	1500 rpm
Nozzle opening pressure	180 bar

Table 3. Uncertainty measurements.

Measurements	Instrument	Uncertainty
CO_2	Gas analyzer	±1.0%
NO_x	Gas analyzer	±5 ppm
UHC	Gas analyzer	±0.5 ppm
rpm	Speed indicator	±2%
Load	Dynamometer	±0.5%
Fuel consumption	Fuel Burette	±1%
BTE		±1.5%
Power		±1%
BSFC		±1.5%

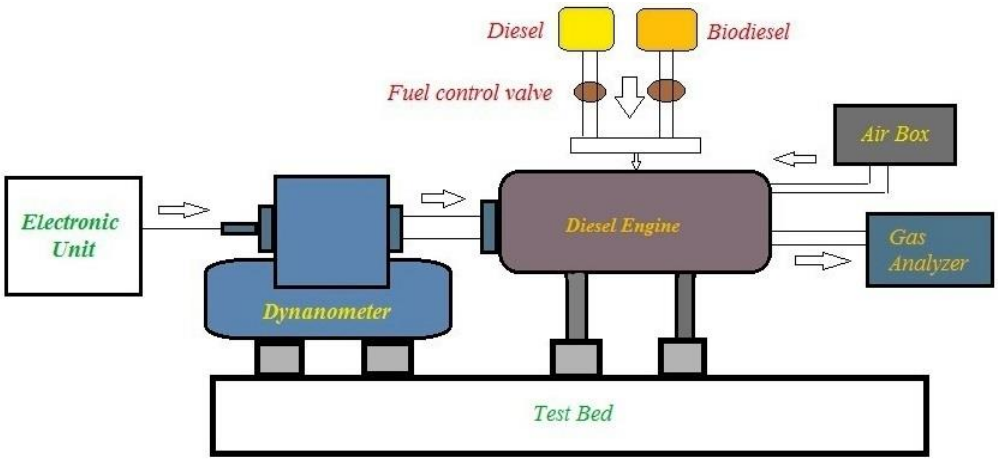

Figure 1. Schematic form of the engine test rig.

3. Artificial Neural Network (ANN)

Preprocessing, and Modeling of ANN

A computational or mathematical framework that resembles the functionalities of a human neuronal system is referred to as an artificial neural network (ANN) [31–33]. ANNs are computational tools that allow doing operations such as memorizing, determining, inferring, and learning. Neurons are the fundamental building blocks of an ANN. By providing a specific proportion of data set (input-output), they can keep updating network architecture based on the data which flows via the structure throughout the training phase [34]. Owing to its nonlinear attributes, ANN can be effectively used in processes to confront tasks with complicated mathematical relationships [35,36].

The data acquired during stable experimental trials was used to create an ANN model. Figure 2 illustrates the suggested ANN strategy for forecasting the CI engine attributes (emissions and performance) using spirulina blends (SB100, SB80, SB65, SB50, SB35, SB20, and SB0). The effectiveness of an ANN is determined by the information it is provided with, therefore scaling input and output information is crucial. The MinMaxScaler (Equation (1)) preprocessing technique [37] was used to normalize the output and input variables. Normalization helps in to equally distribute the importance of input and output data, otherwise, input and output variables with large values become dominant according to fewer values during ANN training.

$$X_{Pre-processing} = \frac{X - X_{min}}{X_{max} - X_{min}} \quad (1)$$

where X_{min} and X_{max} is the minimum and the maximum value of the parameters. X is the value of the parameter to be normalized. The data set normalized in the 0 to 1 range. The data set was chosen at random in the proportions of 20%, 60%, and 20%, for model testing, training, and validation, respectively. Python was used to build an ANN model, utilizing the Keras framework and Tensor flow [38] as the back-end. The ANN network constructed in Python is assessed for several scenarios when varying the training (activation) functions, optimizer, epochs, and the number of network neurons in the hidden layer. Here, output variables comprise HC and NO_X in (ppm), CO_2 and BTE in (%), and BSFC in terms of (kg/kWh). BP (brake power) in (kW), Load in (kg), and test fuels are considered input variables. Figure 3 displays a schematic representation of the proposed ANN architecture, modeled for forecasting CI engine attributes. An optimizer is an algorithm that modifies the attributes of the neural network, such as weights and learning rate, to reduce the losses. The various optimizer evaluated are Adam (a stochastic gradient descent technique based on an adaptive estimate of second and first-order moments), Nadam (optimizer with Nesterov momentum), and Adagrad (optimizer with specific learning rates). The varied transfer or activation functions analyzed are Softmax (output vector are in range (0, 1)), Relu (returns 0 and maximum value), and Sigmoid (returns values between 0 and 1). The activation function determines the output of a neural network model.

The number of network neurons in the hidden layer varied from 8 to 32 with an interval of 8 neurons (i.e., 8, 16, 24, and 32). Throughout the ANN analysis, the single hidden layer was considered, and the number of epochs varied from 200 to 500 with an interval of 100 epochs (i.e., 200, 300, 400, and 500). To generate the associated outputs, the trained ANN network was simulated for all inputs. The r (Correlation Coefficient) and *MSE* (Mean Squared Error) are regarded as network evaluation metrics. To evaluate the direction and strength of the relationship among variables, the r was used. The positive (upwards) and negative (downwards) signs indicate the direction of the relationship. Values ranging from 0.7 to 1.0, 0.3 to 0.7, and 0 to 0.3 are considered to have, respectively, strong, moderate, and weak correlations [39]. The network with the least validation error (loss) is recommended. The best line fit is indicated by a value that is closer to 0. ANN network analysis comprises the following:

- Defining input and output parameters;
- Preprocessing of data (output and input);
- Defining optimizer, transfer function, number of neurons in the hidden layer, and number of epochs;
- Step 1: Adam optimizer with sigmoid transfer function was chosen and evaluated for a varied number of neurons in hidden layers and epochs. By keeping adam optimizer and sigmoid transfer function constant, for each neuron in the hidden layer, four iterations were executed;
- Step 2: Tabulation and plotting of corresponding data (Training *MSE* and r, Validation *MSE* and r of output variables);
- Step 1 and Step 2 were repeated for the Nadam optimizer with a Softmax transfer function and Adagrad optimizer with the Relu transfer function;

- The following equations were used to assess *MSE*, *r* [40], and softmax:

$$MSE = \frac{1}{n}\sum_{i=1}^{n}(T_i - O_i) \tag{2}$$

$$r = \sqrt{1 - \left(\frac{\sum_{i=1}^{n}(T_i - O_i)^2}{\sum_{i=1}^{n} O_i{}^2}\right)} \tag{3}$$

$$\sigma(Z_i) = \frac{e^{z_i}}{\sum_{j=1}^{k} ez_j} \tag{4}$$

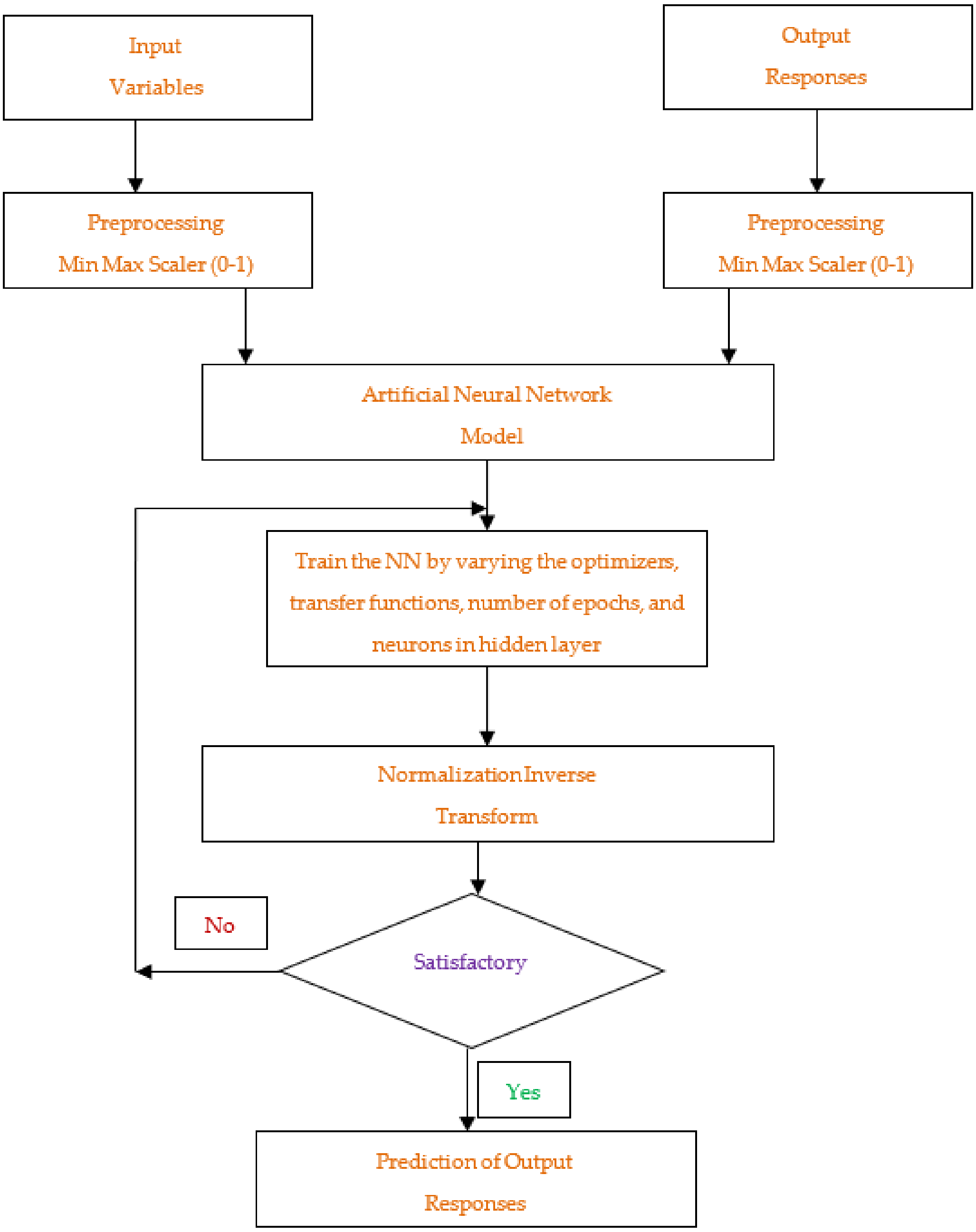

Figure 2. Suggested ANN model strategy.

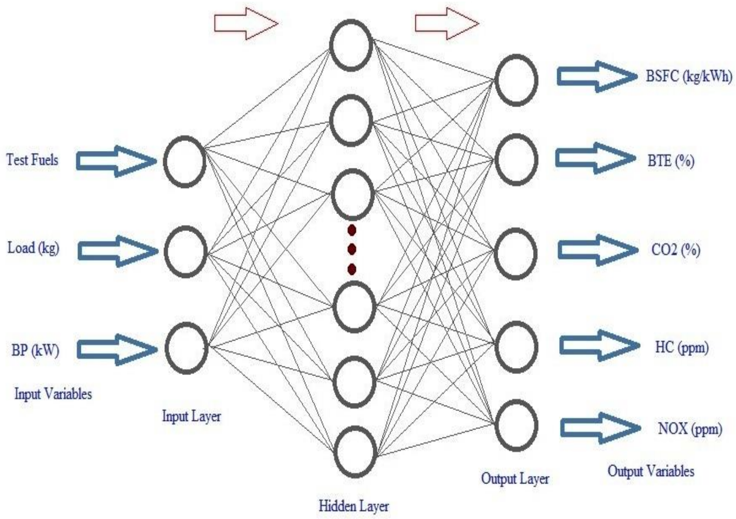

Figure 3. Proposed ANN model configuration.

4. Results and Discussion

4.1. Impact of Brake Specific Fuel Consumption

The fuel heating value has a direct impact on the BSFC. For complete combustion, fuel heating value is perhaps the foremost important factor [41]. The amount of energy required to deliver one unit of power is referred to as BSFC. The BSFC is the amount of fuel that an engine must burn every hour to create one kilowatt of energy. The variation of BSFC (kg/kWh) for SB100, SB80, SB65, SB50, SB35, SB20, and SB0 fuels with varying loads is depicted in Figure 4. An upsurge in BSFC was observed for spirulina bio-diesel blends owing to its reduced brake torques induced by the lower energy content of biodiesel. As shown in Figure 4, as the load enhances, the BSFC for all test fuels declines, owing to increase burning efficiency. The graph depicts that the BSFC for diesel is the lowest. As the proportion of spirulina in baseline fuel (diesel) enhances, BSFC increases. Preceding research reveals an identical behavior to the result [42]. The surge in BSFC was observed to be 4.75% for SB 20 in contrast with SB 0 (diesel) at full load. BSFC (kg/kWh) was noticed to be 0.6212, 0.5732, 0.52117, 0.4488, 0.4122, 0.3782, and 0.36104 for SB100, SB80, SB65, SB50, SB35, SB20, and SB0, respectively, at full load.

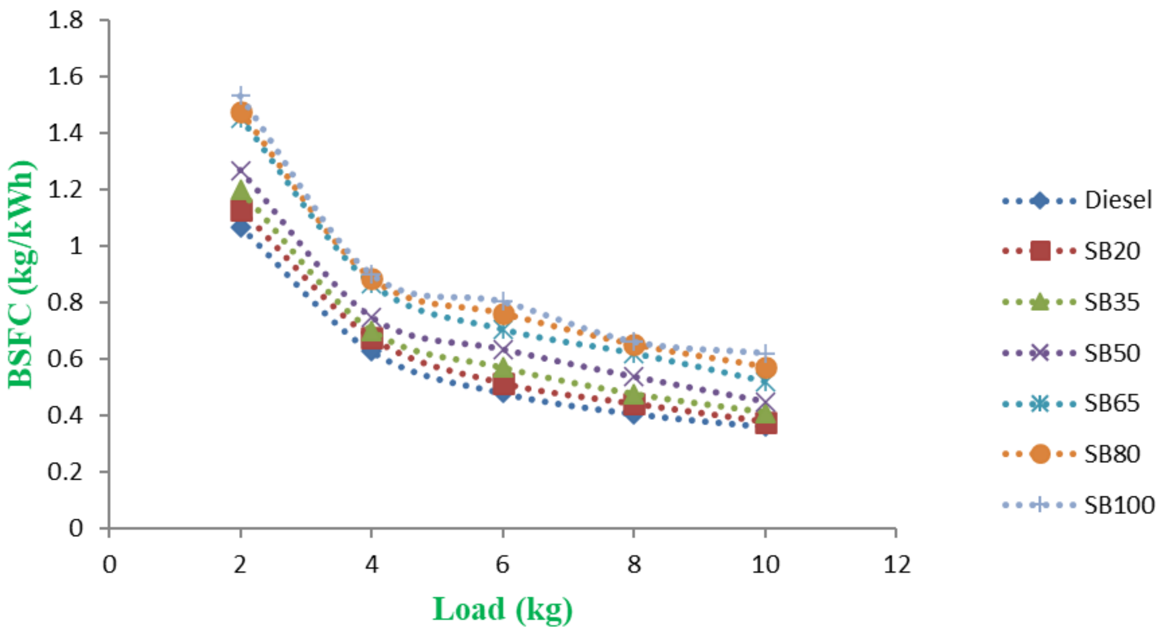

Figure 4. Deviation of BSFC with load.

4.2. Impact of Brake Thermal Efficiency

As depicted in Figure 5, the variation of BTE (%) for SB100, SB80, SB65, SB50, SB35, SB20, and SB0 fuels with varying loads. It is the ratio of brake power to the calorific value and mass of the fuels consumed. As seen in Figure 5, BTE gradually reduced with an upsurge in spirulina bio-diesel concentration in baseline fuel and improved with enhanced engine load. Owing to the lower calorific value, a surge in the BSFC of test fuels leads to reduced BTE [4]. For the majority of engine loads, the BTE and BSFC for SB0 (diesel) was noticed to be higher and lowered in contrast to spirulina blends. An equivalent pattern in other investigators' conclusions [43,44]. BTE dwindled by 3.61% for SB 20 contrasted with SB 0 (diesel) at full load. The minimum BTE is 19.16% which is obtained at SB100.

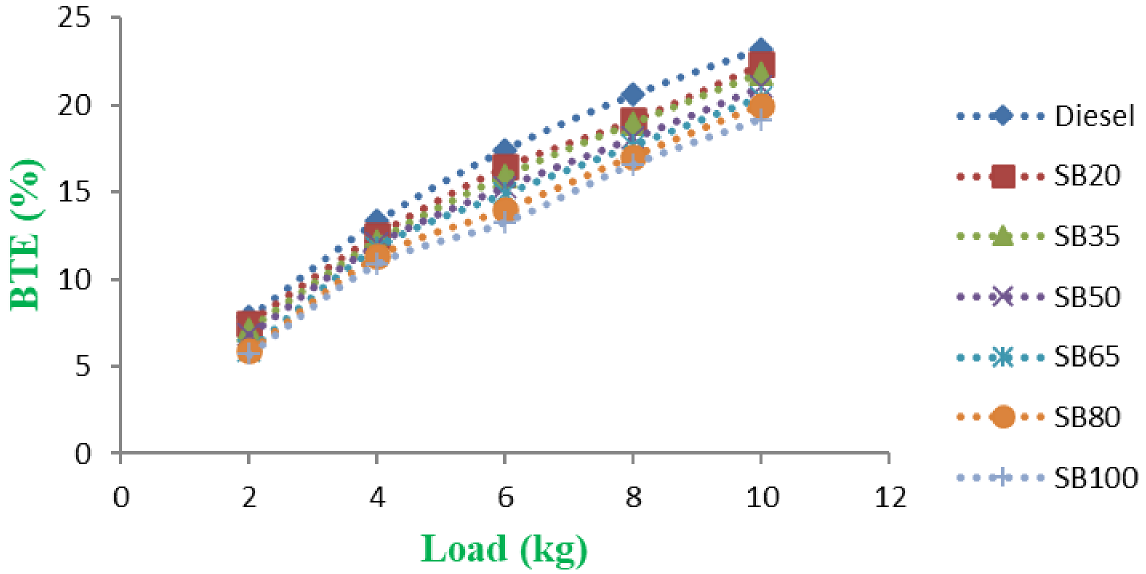

Figure 5. Deviation of BTE with the load.

4.3. Impact of Carbon Dioxide (CO_2) Emissions

The stringent environmental guidelines are minimizing greenhouse gas emissions from many fields of automotive fuels. CO_2 (%) concentrations play a pivotal influence in the formation of ozone. CO_2 effluents from the exhaust are affected by a variety of parameters, particularly engine speed, O_2 concentration in the fuel, compression ratio, viscosity, and combustion process within the cylinder [15]. CO_2 pollutants are emitted when carbon constituents are burned precisely and entirely [27]. CO_2 is emitted as a result of complete combustion. Figure 6 illustrates the CO_2 concentrations (%) for SB100, SB80, SB65, SB50, SB35, SB20, and SB0 fuels with varied loads. It is apparent from the graph there's an upsurge in the CO_2 concentrations when utilizing higher spirulina bio-diesel compositions. CO_2 concentrations were noticed to be significantly higher in spirulina bio-diesel mixtures as opposed to SB0, due to the higher amount of oxygen concentration in the biodiesel. Prior investigations reveal similar findings [41]. The CO_2 concentration in the SB20 improved by 2.83% in comparison to SB0 at full load. The maximum value of CO_2 was observed at SB100 (increased by 19.52%) compared with diesel.

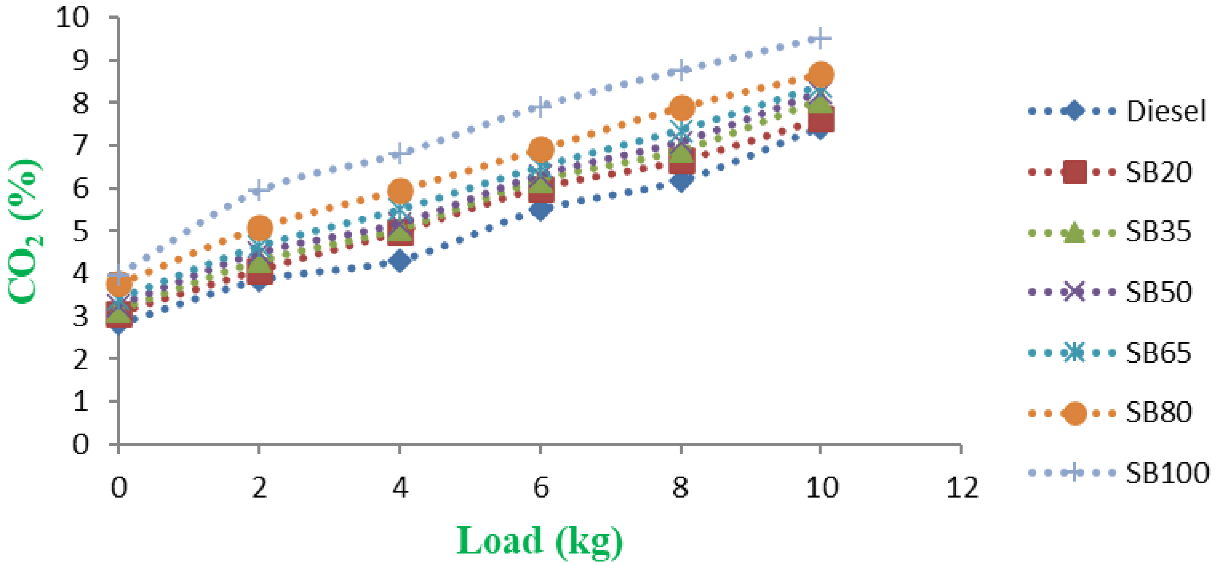

Figure 6. Deviation of CO_2 with the load.

4.4. Impact of Unburnt Hydrocarbons

HC concentrations (ppm) for SB100, SB80, SB65, SB50, SB35, SB20, and SB0 fuels with varying loads are depicted in Figure 7. Since there is insufficient O_2 for complete combustion, HC formed as a result of incomplete oxidation [45]. The concentration of HC is influenced by fuel-spray attributes, fuel properties, and operating conditions of an engine. As may be seen from the plot, due to the increased O_2 moiety available in spirulina bio-diesel, which aids to complete combustion, HC emissions for the spirulina blends (SB100, SB80, SB65, SB50, SB35, and SB20) were lower relative to SB0 (diesel). As the spirulina bio-diesel proportion in a mixture enhanced, HC declined. As a consequence, the engine fueled with spirulina bio-diesel (SB100) emitted the least amount of HC when contrasted to SB80, SB65, SB50, SB35, SB20, and SB0. Another aspect that contributed to the reduction in HC was the higher CN of spirulina bio-diesel compared to diesel, which leads to a shorter ignition delay. The findings acquired corresponded to those presented by [44].

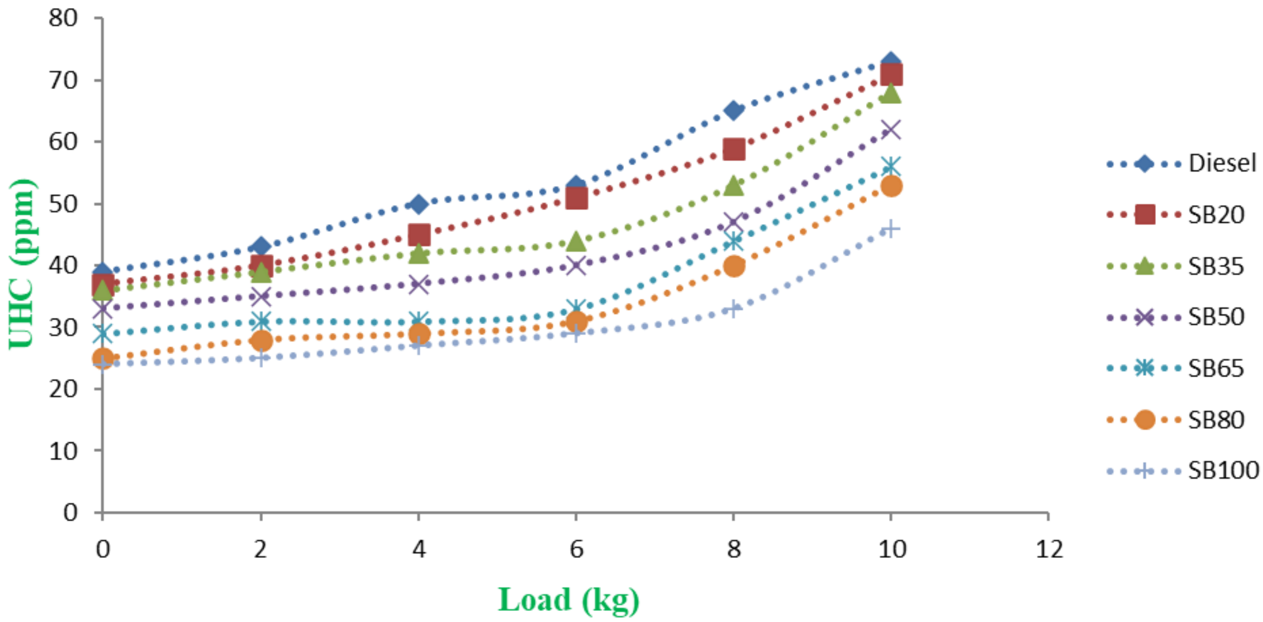

Figure 7. Deviation of UHC with the load.

4.5. Impact of Nitrogen Oxides (NO_X) Emissions

NO_x remains a significant key engine exhaust byproduct that must be minimized. Pollutant formation is heavily influenced by fuel distribution and how it varies with time due to mixing. The distribution of fuel in the cylinder is often irregular in CI engines. Mixture homogeneity, O_2 concentrations, combustion temperature, and pressure, CN, ignition delay, flame temperature, fuel attributes, and injection timing are factors that influence NO_x emissions [22]. NO_X occurs in an irregular high-temperature zone and forms a rate upsurge in areas near stoichiometry. As a consequence, NO_X is mainly influenced by fuel O_2 concentration and the temperature of combustion [21]. Change of NO_X concentrations (ppm) for SB100, SB80, SB65, SB50, SB35, SB20, and SB0 fuels with varying loads is represented in Figure 8. It is apparent from the graph there's a downturn in the NO_x concentrations when utilizing higher spirulina bio-diesel compositions. NO_X concentrations were noticed to be significantly higher in baseline fuel (SB0) as opposed to spirulina bio-diesel mixtures (SB100, SB80, SB65, SB50, SB35, and SB20). Similar findings were acquired by [11,46]. When contrasted to SB0 (diesel), NO_X emissions for SB100 and SB20 are 15.65% and 3.82% lower at full load, respectively.

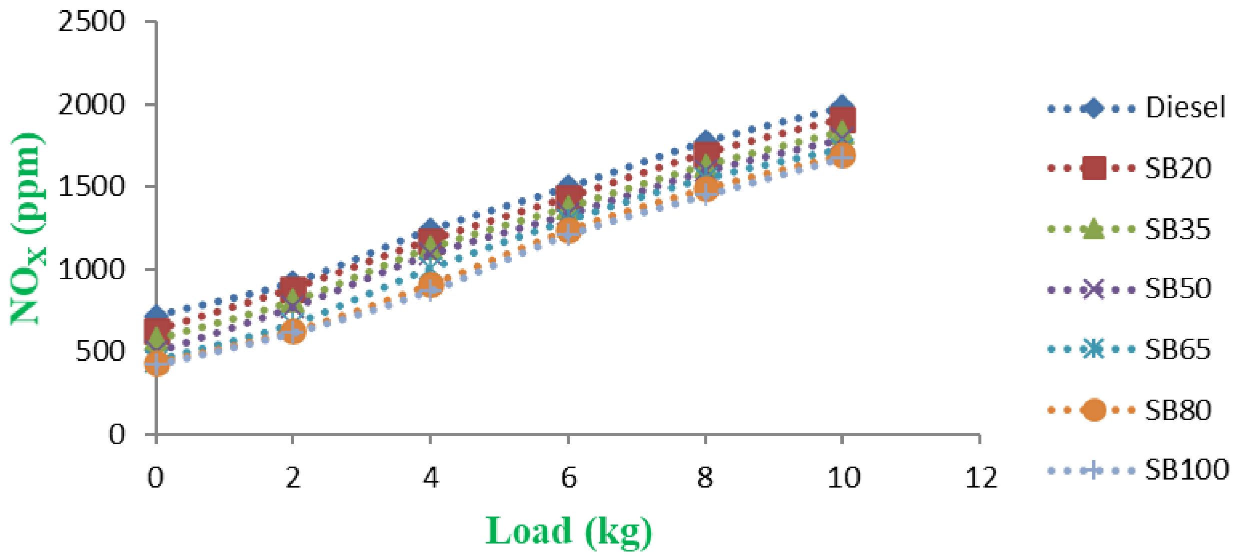

Figure 8. Deviation of NO_X with the load.

4.6. Analysis of ANN

For various optimizers and activation functions, ANN network training was performed for varied epochs and numbers of neurons, and the outcomes obtained were summarized in Table 4. Contrasted to other training optimizers and activation functions, Adam optimizer with sigmoid activation function for hidden layer exhibits the best r and least validation mean squared error. The optimum configuration of the network is shown in Table 5. Figures 9 and 10 illustrate the change of r value and MSE loss of optimum network configuration for training and validation data of output variables, with the number of epochs. From Figure 9 it was observed that with the increase in the number of epochs the correlation coefficient of output variables (NO_X, HC, CO_2, BTE, and BSFC) tends to be 1, indicating a strong correlation. With the increase in the number of epochs, the MSE loss decreases as seen in Figure 10. The train and validation loss of output variables were almost identical. The number of neurons required for MSE to be least is observed to be 32 in this study. All output variables are significantly connected with input variables, as per the trend of the r. The optimum network prediction for test cases is recorded and presented, together with the associated experimentally obtained results as in Figure 11. The r and MSE values of CI engine attributes are found to be 0.99928, 0.99588, 0.99848, 0.99949, and 0.99322, and 0.00013, 0.00060, 0.00021, 0.00011, and 0.00104 for NO_X, HC, CO_2, BTE, and BSFC, respectively, as observed in Figure 11.

Table 4. r and MSE values of output responses.

Optimizer	Transfer Function	Number of Epochs	Number of Neurons in Hidden Layer	Attributes	Train. MSE	Val. MSE	Over All MSE Loss		Train. r:	Val. r:
					Loss	Loss	Train.	Val.		
Adam	Sigmoid	200	8	BSFC	0.0086	0.01232	0.00269	0.00497	0.9423	0.84607
				BTE	0.00083	0.00097			0.99596	0.99203
				CO_2	0.00108	0.00246			0.99206	0.97945
				HC	0.00234	0.00873			0.98389	0.95286
				NO_X	0.00058	0.00037			0.99681	0.99729
Adam	Sigmoid	300	8	BSFC	0.00511	0.02273	0.00148	0.00618	0.96878	0.72042
				BTE	0.00044	0.00069			0.99788	0.99457
				CO_2	0.00052	0.00075			0.99618	0.99546
				HC	0.00105	0.00621			0.99283	0.97256
				NO_X	0.00029	0.0005			0.99842	0.99606
Adam	Sigmoid	400	8	BSFC	0.02134	0.03784	0.0056	0.01073	0.85104	0.50068
				BTE	0.00055	0.00131			0.99735	0.99386
				CO_2	0.00126	0.00104			0.99072	0.99369
				HC	0.00425	0.0126			0.97048	0.9483
				NO_X	0.00061	0.00089			0.99661	0.99751
Adam	Sigmoid	500	8	BSFC	0.00206	0.01015	0.00072	0.003	0.98637	0.92099
				BTE	0.0002	0.00031			0.99905	0.99839
				CO_2	0.00027	0.00054			0.99802	0.99177
				HC	0.00058	0.00289			0.99599	0.98256
				NO_X	0.00051	0.0011			0.99718	0.9964
Adam	Sigmoid	200	16	BSFC	0.02611	0.04097	0.00594	0.00998	0.81547	0.36112
				BTE	0.00021	0.00032			0.99899	0.9968
				CO_2	0.0005	0.00088			0.99631	0.99342
				HC	0.00209	0.00742			0.98568	0.96278
				NO_X	0.00082	0.00033			0.99549	0.99999
Adam	Sigmoid	300	16	BSFC	0.01394	0.02282	0.00358	0.00702	0.90453	0.69879
				BTE	0.00029	0.00048			0.9986	0.99582
				CO_2	0.00063	0.00116			0.99539	0.99342
				HC	0.00254	0.01016			0.98245	0.95267
				NO_X	0.0005	0.00047			0.99725	0.99615
Adam	Sigmoid	400	16	BSFC	0.00579	0.02621	0.00195	0.00817	0.96209	0.67509
				BTE	0.00039	0.00035			0.9981	0.99693
				CO_2	0.00117	0.00226			0.99139	0.99753
				HC	0.00213	0.01133			0.98532	0.95155
				NO_X	0.00025	0.00069			0.99863	0.99628
Adam	Sigmoid	500	16	BSFC	0.00137	0.00984	0.00046	0.00267	0.99099	0.89962
				BTE	0.00011	0.00033			0.99948	0.99653
				CO_2	0.00023	0.00038			0.99832	0.99328
				HC	0.00048	0.0027			0.99674	0.97969
				NO_X	0.00011	0.00012			0.9994	0.99903
Adam	Sigmoid	200	24	BSFC	0.03194	0.05353	0.00714	0.01254	0.77304	0.08641
				BTE	0.00022	0.00049			0.99896	0.99558
				CO_2	0.00067	0.00147			0.99509	0.98629
				HC	0.00249	0.00706			0.98305	0.95967
				NO_X	0.00036	0.00015			0.998	0.99933
Adam	Sigmoid	300	24	BSFC	0.00782	0.02142	0.00226	0.00686	0.94742	0.71643
				BTE	0.00042	0.00056			0.99795	0.99473
				CO_2	0.00052	0.00097			0.99617	0.99459
				HC	0.00237	0.01127			0.98368	0.94964
				NO_X	0.00015	0.0001			0.99917	0.99921
Adam	Sigmoid	400	24	BSFC	0.00769	0.02733	0.00256	0.00892	0.94828	0.65893
				BTE	0.00068	0.00063			0.99672	0.99615
				CO_2	0.0009	0.00213			0.99339	0.99789
				HC	0.0033	0.01386			0.97723	0.94008
				NO_X	0.00025	0.00066			0.99861	0.99674
Adam	Sigmoid	500	24	BSFC	0.00088	0.0038	0.00042	0.00181	0.99424	0.96032
				BTE	0.00006	0.00018			0.99972	0.99862
				CO_2	0.00028	0.00036			0.99793	0.98916
				HC	0.00072	0.00426			0.99505	0.97595
				NO_X	0.00016	0.00016			0.99914	0.99889
Adam	Sigmoid	200	32	BSFC	0.03306	0.05259	0.00744	0.01273	0.76369	0.15619
				BTE	0.00053	0.00067			0.99745	0.99462
				CO_2	0.00101	0.00242			0.99256	0.99565
				HC	0.00209	0.00781			0.98557	0.96626
				NO_X	0.00049	0.00014			0.99731	0.99905
Adam	Sigmoid	300	32	BSFC	0.02158	0.03714	0.00513	0.01025	0.85291	0.4619
				BTE	0.0003	0.00029			0.99854	0.99711
				CO_2	0.00056	0.00101			0.99586	0.99513
				HC	0.00298	0.01263			0.97943	0.94433
				NO_X	0.00025	0.00015			0.9986	0.99883

Table 4. *Cont.*

Optimizer	Transfer Function	Number of Epochs	Number of Neurons in Hidden Layer	Attributes	Train. MSE	Val. MSE	Over All MSE Loss		Train. r:	Val. r:
					Loss	Loss	Train.	Val.		
Adam	Sigmoid	400	32	BSFC	0.00073	0.00674	0.0004	0.0023	0.99539	0.94095
				BTE	0.0001	0.0002			0.99952	0.99793
				CO_2	0.00025	0.00054			0.99814	0.99364
				HC	0.00068	0.00385			0.99535	0.98254
				NO_X	0.00023	0.00016			0.99875	0.99969
Adam	*Sigmoid*	*500*	*32*	*BSFC*	*0.00075*	*0.00331*	*0.00039*	*0.00175*	*0.99512*	*0.96477*
				BTE	*0.00007*	*0.0002*			*0.99967*	*0.99846*
				CO_2	*0.00019*	*0.00049*			*0.99863*	*0.99203*
				HC	*0.00081*	*0.00488*			*0.99446*	*0.97394*
				NO_X	*0.00013*	*0.00017*			*0.99927*	*0.99866*
Nadam	Softmax	200	8	BSFC	0.01359	0.03844	0.00554	0.01206	0.9478	0.52292
				BTE	0.00093	0.00102			0.99723	0.99672
				CO_2	0.00868	0.0042			0.99145	0.98368
				HC	0.00271	0.01411			0.98899	0.9545
				NO_X	0.00177	0.00252			0.9975	0.98849
Nadam	Softmax	300	8	BSFC	0.00442	0.01707	0.00976	0.0251	0.97099	0.79434
				BTE	0.00479	0.01118			0.99775	0.99096
				CO_2	0.01485	0.02879			0.9933	0.98269
				HC	0.0187	0.05233			0.98798	0.96139
				NO_X	0.00606	0.01615			0.99674	0.98703
Nadam	Softmax	400	8	BSFC	0.0062	0.0397	0.00397	0.01413	0.9828	0.55435
				BTE	0.00335	0.00346			0.99921	0.99803
				CO_2	0.00323	0.00713			0.99516	0.97772
				HC	0.00344	0.01474			0.99471	0.97046
				NO_X	0.00361	0.00562			0.99876	0.99592
Nadam	Softmax	500	8	BSFC	0.00416	0.00941	0.00443	0.00993	0.98428	0.90226
				BTE	0.00477	0.0073			0.99848	0.98826
				CO_2	0.00307	0.00976			0.99305	0.97928
				HC	0.005	0.01465			0.99305	0.9802
				NO_X	0.00518	0.00852			0.99833	0.99039
Nadam	Softmax	200	16	BSFC	0.01921	0.02933	0.00899	0.01087	0.97023	0.73502
				BTE	0.00771	0.00732			0.99708	0.99178
				CO_2	0.00153	0.0019			0.99556	0.99295
				HC	0.00577	0.00747			0.98268	0.95034
				NO_X	0.01073	0.00834			0.99635	0.99307
Nadam	Softmax	300	16	BSFC	0.00832	0.02024	0.00382	0.0109	0.98117	0.80768
				BTE	0.00312	0.00662			0.99838	0.98905
				CO_2	0.00283	0.01035			0.99637	0.98672
				HC	0.00178	0.00989			0.99175	0.9592
				NO_X	0.00306	0.00741			0.99856	0.99244
Nadam	Softmax	400	16	BSFC	0.00781	0.01739	0.00426	0.00992	0.98681	0.87054
				BTE	0.00452	0.00749			0.99889	0.99032
				CO_2	0.00148	0.00501			0.99797	0.98655
				HC	0.00276	0.01272			0.99487	0.9662
				NO_X	0.00473	0.00698			0.99863	0.9951
Nadam	Softmax	500	16	BSFC	0.00597	0.02053	0.00483	0.01243	0.99016	0.82648
				BTE	0.00448	0.00594			0.9988	0.99357
				CO_2	0.0005	0.00287			0.99812	0.99373
				HC	0.00732	0.02445			0.99471	0.96771
				NO_X	0.00586	0.00835			0.99867	0.99789
Nadam	Softmax	200	24	BSFC	0.01214	0.02655	0.00376	0.00909	0.97054	0.6949
				BTE	0.00192	0.00124			0.99701	0.99206
				CO_2	0.00039	0.00211			0.99769	0.99284
				HC	0.00206	0.01429			0.99001	0.9524
				NO_X	0.00227	0.00125			0.99768	0.99433
Nadam	Softmax	300	24	BSFC	0.014	0.02197	0.00441	0.00703	0.9814	0.74216
				BTE	0.00324	0.00315			0.99825	0.99391
				CO_2	0.00099	0.00161			0.9974	0.99468
				HC	0.00068	0.00622			0.9955	0.97638
				NO_X	0.00315	0.00222			0.9986	0.9958
Nadam	Softmax	400	24	BSFC	0.01542	0.02914	0.00574	0.0119	0.98459	0.87196
				BTE	0.00563	0.01167			0.99848	0.98877
				CO_2	0.00265	0.00547			0.99808	0.99796
				HC	0.00092	0.00566			0.99589	0.97293
				NO_X	0.00407	0.00753			0.99894	0.99651
Nadam	Softmax	500	24	BSFC	0.00164	0.022	0.00199	0.01008	0.99095	0.74711
				BTE	0.00122	0.00303			0.99899	0.98921
				CO_2	0.00143	0.00448			0.99816	0.98602
				HC	0.004	0.01606			0.99589	0.96192
				NO_X	0.00164	0.0048			0.99889	0.99327

Table 4. *Cont.*

Optimizer	Transfer Function	Number of Epochs	Number of Neurons in Hidden Layer	Attributes	Train. MSE	Val. MSE	Over All MSE Loss		Train. r:	Val. r:
					Loss	Loss	Train.	Val.		
Nadam	Softmax	200	32	BSFC	0.00444	0.03051	0.00521	0.01018	0.97672	0.63954
				BTE	0.00687	0.00558			0.9984	0.99043
				CO_2	0.00717	0.00366			0.99636	0.9966
				HC	0.00293	0.00784			0.98793	0.95762
				NO_X	0.00465	0.00331			0.99837	0.99522
Nadam	Softmax	300	32	BSFC	0.00984	0.01614	0.00381	0.00557	0.98572	0.82234
				BTE	0.00307	0.00288			0.99855	0.99331
				CO_2	0.0017	0.00134			0.99817	0.99279
				HC	0.00119	0.00497			0.99353	0.97268
				NO_X	0.00325	0.0025			0.99903	0.99676
Nadam	Softmax	400	32	BSFC	0.00392	0.01958	0.00346	0.01143	0.99077	0.83959
				BTE	0.00306	0.00674			0.99899	0.98818
				CO_2	0.00483	0.01014			0.99864	0.99632
				HC	0.00249	0.01499			0.99572	0.96501
				NO_X	0.003	0.0057			0.99913	0.99635
Nadam	Softmax	500	32	BSFC	0.00151	0.01375	0.00196	0.00417	0.99354	0.83431
				BTE	0.00145	0.00173			0.99911	0.99288
				CO_2	0.00087	0.00078			0.99875	0.99589
				HC	0.00414	0.00351			0.99569	0.97439
				NO_X	0.00186	0.0011			0.99923	0.99805
Adagrad	Relu	200	8	BSFC	0.06691	0.05035	0.02132	0.01774	0.34902	0.53797
				BTE	0.01225	0.01094			0.9397	0.9522
				CO_2	0.01186	0.00866			0.90866	0.82812
				HC	0.00848	0.01028			0.94016	0.91711
				NO_X	0.00708	0.00844			0.9632	0.95271
Adagrad	Relu	300	8	BSFC	0.06728	0.04799	0.01579	0.01281	0.34207	0.28044
				BTE	0.00411	0.00507			0.97995	0.99154
				CO_2	0.00103	0.00226			0.99268	0.96619
				HC	0.00333	0.00631			0.97771	0.95808
				NO_X	0.00323	0.00242			0.98218	0.99713
Adagrad	Relu	400	8	BSFC	0.0674	0.0447	0.01638	0.01107	0.34413	0.38635
				BTE	0.00427	0.00457			0.97915	0.99054
				CO_2	0.00153	0.00131			0.98872	0.99051
				HC	0.00789	0.00396			0.94452	0.97742
				NO_X	0.0008	0.00081			0.99559	0.99654
Adagrad	Relu	500	8	BSFC	0.04943	0.06764	0.01335	0.01683	0.7185	−0.5345
				BTE	0.00472	0.00384			0.97693	0.96884
				CO_2	0.00363	0.00422			0.97296	0.94953
				HC	0.00785	0.00818			0.94478	0.94958
				NO_X	0.00111	0.00026			0.99387	0.99845
Adagrad	Relu	200	16	BSFC	0.05379	0.05165	0.01385	0.01258	0.62853	0.06749
				BTE	0.00437	0.00408			0.97882	0.98665
				CO_2	0.00301	0.00133			0.9777	0.99282
				HC	0.00646	0.00518			0.95478	0.97201
				NO_X	0.00163	0.00066			0.99098	0.99832
Adagrad	Relu	300	16	BSFC	0.061	0.07195	0.01474	0.01696	0.47368	−0.42298
				BTE	0.00436	0.00455			0.9788	0.99563
				CO_2	0.00156	0.00372			0.98854	0.99239
				HC	0.00526	0.00457			0.96387	0.97707
				NO_X	0.00152	0.00002			0.9916	0.99998
Adagrad	Relu	400	16	BSFC	0.0637	0.07373	0.01518	0.01787	0.43457	−0.64301
				BTE	0.00363	0.005			0.9823	0.98471
				CO_2	0.0022	0.00109			0.98386	0.97084
				HC	0.00566	0.00888			0.96048	0.95955
				NO_X	0.00071	0.00063			0.99607	0.99884
Adagrad	Relu	500	16	BSFC	0.05292	0.06428	0.01305	0.01739	0.60676	−0.14604
				BTE	0.00513	0.00592			0.97486	0.98378
				CO_2	0.0013	0.00135			0.99043	0.95878
				HC	0.00477	0.0149			0.96679	0.9272
				NO_X	0.00112	0.00047			0.9938	0.99859
Adagrad	Relu	200	24	BSFC	0.05528	0.05445	0.01364	0.0157	0.61015	0.0156
				BTE	0.0045	0.00675			0.97798	0.97732
				CO_2	0.00389	0.00289			0.97107	0.98276
				HC	0.00385	0.01424			0.9733	0.93214
				NO_X	0.00066	0.00019			0.99638	0.99959
Adagrad	Relu	300	24	BSFC	0.05563	0.06067	0.01326	0.01512	0.58647	−0.1716
				BTE	0.00226	0.00185			0.98906	0.99573
				CO_2	0.00179	0.00324			0.98672	0.99923
				HC	0.00455	0.00741			0.96848	0.94134
				NO_X	0.00208	0.00242			0.98866	0.99463

Table 4. *Cont.*

Optimizer	Transfer Function	Number of Epochs	Number of Neurons in Hidden Layer	Attributes	Train. MSE	Val. MSE	Over All MSE Loss		Train. r:	Val. r:
					Loss	Loss	Train.	Val.		
Adagrad	Relu	400	24	BSFC	0.06072	0.06219	0.01441	0.01609	0.49497	−0.26716
				BTE	0.00503	0.00578			0.97541	0.99
				CO_2	0.00114	0.00186			0.99164	0.99895
				HC	0.00428	0.00993			0.97035	0.93742
				NO_X	0.00087	0.0007			0.99521	0.99496
Adagrad	Relu	500	24	BSFC	0.06106	0.06679	0.01449	0.01772	0.48641	−0.35244
				BTE	0.00494	0.00498			0.97582	0.99074
				CO_2	0.00108	0.00164			0.99204	0.96514
				HC	0.00453	0.01464			0.96851	0.92427
				NO_X	0.00086	0.00055			0.99523	0.99985
Adagrad	Relu	200	32	BSFC	0.06148	0.05739	0.01474	0.01574	0.47624	0.29582
				BTE	0.00523	0.00305			0.97444	0.99025
				CO_2	0.00117	0.00179			0.99162	0.98774
				HC	0.00444	0.01543			0.96923	0.92201
				NO_X	0.00139	0.00103			0.9923	0.99568
Adagrad	Relu	300	32	BSFC	0.05007	0.05915	0.01228	0.01494	0.67119	−0.03018
				BTE	0.00273	0.00324			0.98679	0.99698
				CO_2	0.00171	0.00156			0.98739	0.98397
				HC	0.00587	0.01003			0.95902	0.93103
				NO_X	0.00103	0.00072			0.99428	0.9994
Adagrad	Relu	400	32	BSFC	0.05529	0.06235	0.01261	0.01504	0.57119	−0.21838
				BTE	0.00184	0.00094			0.99107	0.99651
				CO_2	0.00147	0.00179			0.98914	0.97134
				HC	0.00373	0.0097			0.97414	0.94638
				NO_X	0.00074	0.0004			0.99593	0.99942
Adagrad	Relu	500	32	BSFC	0.03947	0.05622	0.01	0.01404	0.78943	−0.12114
				BTE	0.0028	0.00401			0.98639	0.99593
				CO_2	0.00242	0.00167			0.98224	0.9964
				HC	0.00407	0.00791			0.97173	0.9615
				NO_X	0.00123	0.0004			0.99319	0.99762

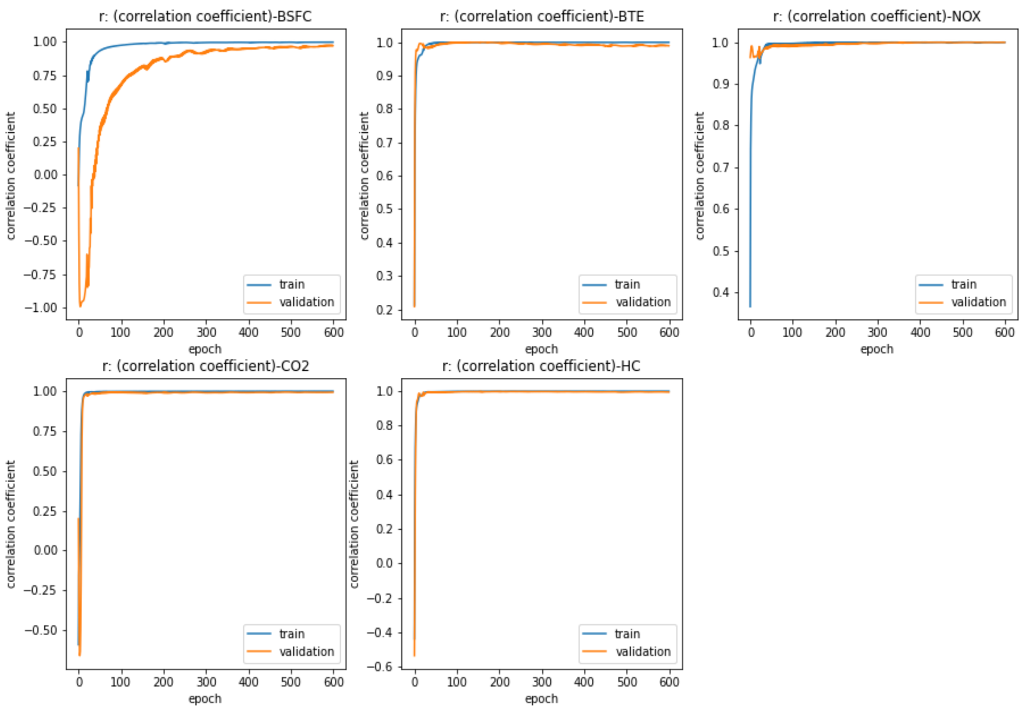

Figure 9. Deviation of r value (train and validation) with the number of epochs for optimum network configuration.

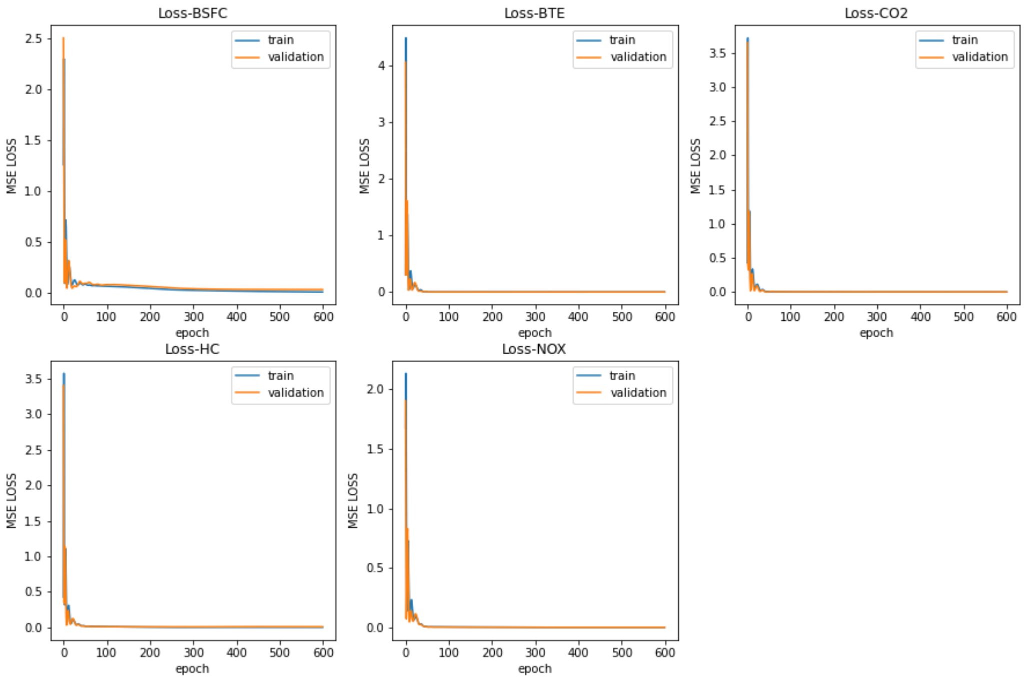

Figure 10. Deviation of MSE loss (train and validation) with the number of epochs for optimum network configuration.

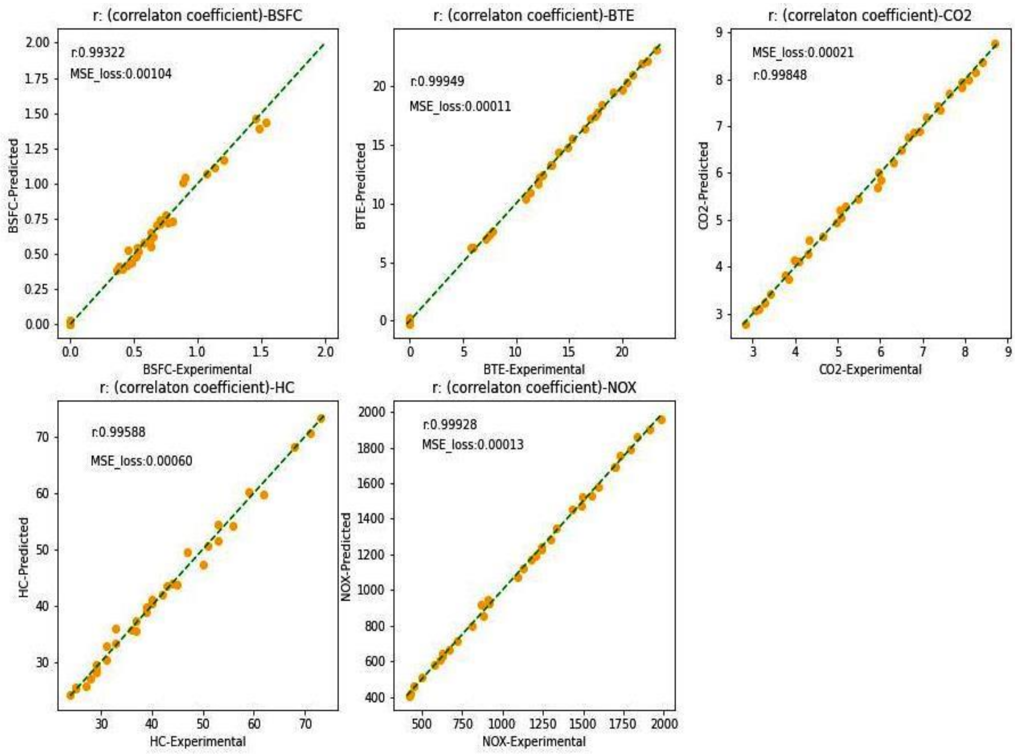

Figure 11. ANN estimations for the output responses (experimental vs. predicted) for optimum network configuration.

Table 5. ANN model optimum configuration.

Output layer neurons	5
Hidden layer neurons	32
Input layer neurons	3
Normalized range	0 to 1
Transfer functions	Sigmoid
Optimizer	Adam
Evaluation metrics	r and MSE
Number of epochs	500
Preprocessing	MinMax Scaler

5. Main Findings

- SB100 depicted a significant reduction in NO_X and thermal efficiency. Bio-diesel derived from micro-algae spirulina, among one of the alternative energy sources that can be utilized instead of diesel, has a significant prospective for lowering NO_X concentrations;
- As opposed to the spirulina blend SB0 has decreased specific fuel consumption;
- For prediction of CI Engine attributes ANN framework utilizing python with the Tensor flow as backend and Keras framework was implemented;
- Optimizers such as adam, nadam, and adagrad were evaluated and adam was found to be the optimum.

6. Conclusions

CI engine attributes and ANN model of a 17.5 compression ratio diesel engine fueled with varied spirulina blends SB100, SB80, SB65, SB50, SB35, SB20, and SB0 were analyzed. The preceding points are the conclusions from this study's findings.

- The outcomes demonstrated a reduction in BTE, HC, and NO_X concentrations when micro-algae spirulina blends were applied; however, a rise inCO_2 and BSFC was observed relative to SB0;
- SB100 was found to be the minimum BTE as compared to other blends. SB100 has a substantial impact on reducing NO_X concentrations, but CO_2 enhanced is correlative to diesel (SB0);
- The proposed ANN was a three-layer one that utilized output variables (NO_X, HC, CO_2, BTE, and BSFC) and input variables (load, test fuels, and BP);
- Adam optimizer with sigmoid transfer function was found to be best suited for training the network. The optimum network configuration was composed of 32 neurons in a hidden layer, and the best architecture of ANN was found to be 3-32-5;
- The overall network validation and training MSE loss was found to be 0.00175 and 0.00039, respectively. The experimental results and model outcomes are correlated with each other and revealed that the ANN technique has given optimum results.

Author Contributions: S.C.K.: Conceptualization, Writing—Original Draft, Writing—Review and Editing Investigation. A.K.T.: Conceptualization, Writing—Original Draft, Writing—Review and Editing Investigation. J.R.A.: Conceptualization, Writing—Original Draft, Writing—Review and Editing Investigation. S.K.N.: Conceptualization, Writing—Review and Editing, Supervision. R.S.: Writing—Review and Editing, Supervision; N.P.: Writing—Review and Editing, Supervision; B.T.: Writing—Review and Editing, Funding Acquisition, Supervision.All authors have read and agreed to the published version of the manuscript.

Funding: The APC was funded by Tshwane University of Technology, South Africa.

Institutional Review Board Statement: Not applicable.

Informed Consent Statement: Not applicable.

Data Availability Statement: No data is used in this article.

Conflicts of Interest: The authors declare that they have no competing interest.

Nomenclature

ANN	Artificial Neural Network
BSFC	Brake Specific Fuel Consumption
BTE	Brake Thermal Efficiency
CN	Cetane Number
CO	Carbon-Monoxide
CO_2	Carbon-Dioxide
DI	Direct Injection
MSE	Mean Squared Error
UHC	Unburnt Hydro-Carbons
NO_X	Nitrogen Oxide
O_2	Oxygen
Oi	Output for ith trail case
ppm	Parts per million
r	Correlation Coefficient
TC	Turbo Charged
Ti	Target for ith trial case
Val	Validation
Train	Training
BP	Brake power

References

1. Datta, A.; Mandal, B.K. A Comprehensive Review of Biodiesel as an Alternative Fuel for Compression Ignition Engine. *Renew. Sustain. Energy Rev.* **2016**, *57*, 799–821. [CrossRef]
2. Dwivedi, G.; Sharma, M.P. Prospects of Biodiesel from Pongamia in India. *Renew. Sustain. Energy Rev.* **2014**, *32*, 114–122. [CrossRef]
3. Arunprasad, S.; Balusamy, T. Experimental investigation on the performance and emission characteristics of a diesel engine by varying the injection pressure and injection timing using mixed biodiesel. *Int. J. Green Energy* **2018**, *15*, 376–384. [CrossRef]
4. Singh, D.; Sharma, D.; Soni, S.L.; Sharma, S.; Kumar Sharma, P.; Jhalani, A. A Review on Feedstocks, Production Processes, and Yield for Different Generations of Biodiesel. *Fuel* **2020**, *262*, 116553. [CrossRef]
5. Aro, E.M. From First Generation Biofuels to Advanced Solar Biofuels. *Ambio* **2016**, *45*, 24–31. [CrossRef]
6. Alalwan, H.A.; Alminshid, A.H.; Aljaafari, H.A.S. Promising Evolution of Biofuel Generations. Subject Review. *Renew. Energy Focus* **2019**, *28*, 127–139.
7. Venkatesan, H.; Rose, G.J.J.; Vijayarengan, P.; Sivamani, S.; Krishnan, J.; Thomai, M.P. Predicting the combustion behaviour of compression ignition engine fuelled with biodiesel from Stoechosper mummarginatum, a macro algae. *Environ. Sci. Pollut. Res.* **2021**, *28*, 63464–63479. [CrossRef]
8. Yusri, I.M.; Abdul Majeed, A.P.P.; Mamat, R.; Ghazali, M.F.; Awad, O.I.; Azmi, W.H. A Review on the Application of Response Surface Method and Artificial Neural Network in Engine Performance and Exhaust Emissions Characteristics in Alternative Fuel. *Renew. Sustain. Energy Rev.* **2018**, *90*, 665–686. [CrossRef]
9. Uslu, S. Optimization of Diesel Engine Operating Parameters Fueled with Palm Oil-Diesel Blend: Comparative Evaluation between Response Surface Methodology (RSM) and Artificial Neural Network (ANN). *Fuel* **2020**, *276*, 117990. [CrossRef]
10. Manimaran, R.; Mohanraj, T.; Venkatesan, M. ANN modeling for forecasting of VCR engine performance and emission parameters fuelled with green diesel extracted from waste biomass resources. *Environ. Sci. Pollut. Res.* **2022**, *29*, 51183–51210. [CrossRef]
11. Shrivastava, P.; Salam, S.; Verma, T.N.; Samuel, O.D. Experimental and Empirical Analysis of an IC Engine Operating with Ternary Blends of Diesel, Karanja and Roselle Biodiesel. *Fuel* **2020**, *262*, 116608. [CrossRef]
12. Taghavi, M.; Gharehghani, A.; Nejad, F.B.; Mirsalim, M. Developing a Model to Predict the Start of Combustion in HCCI Engine Using ANN-GA Approach. *Energy Convers. Manag.* **2019**, *195*, 57–69. [CrossRef]
13. Uslu, S.; Celik, M.B. Prediction of Engine Emissions and Performance with Artificial Neural Networks in a Single Cylinder Diesel Engine Using Diethyl Ether. *Eng. Sci. Technol. Int. J.* **2018**, *21*, 1194–1201. [CrossRef]
14. Datta, A.; Mandal, B.K. Engine Performance, Combustion and Emission Characteristics of a Compression Ignition Engine Operating on Different Biodiesel-Alcohol Blends. *Energy* **2017**, *125*, 470–483. [CrossRef]
15. Bueno, A.V.; Pereira, M.P.B.; de Oliveira Pontes, J.V.; de Luna, F.M.T.; Cavalcante, C.L. Performance and Emissions Characteristics of Castor Oil Biodiesel Fuel Blends. *Appl. Therm. Eng.* **2017**, *125*, 559–566. [CrossRef]
16. Al-lwayzy, S.H.; Yusaf, T. Diesel Engine Performance and Exhaust Gas Emissions Using Microalgae Chlorella Protothecoides Biodiesel. *Renew. Energy* **2017**, *101*, 690–701. [CrossRef]

17. Kalsi, S.S.; Subramanian, K.A. Effect of Simulated Biogas on Performance, Combustion and Emissions Characteristics of a Bio-Diesel Fueled Diesel Engine. *Renew. Energy* **2017**, *106*, 78–90. [CrossRef]
18. Can, Ö.; Öztürk, E.; Yücesu, H.S. Combustion and Exhaust Emissions of Canola Biodiesel Blends in a Single Cylinder DI Diesel Engine. *Renew. Energy* **2017**, *109*, 73–82. [CrossRef]
19. Srihari, S.; Thirumalini, S.; Prashanth, K. An Experimental Study on the Performance and Emission Characteristics of PCCI-DI Engine Fuelled with Diethyl Ether-Biodiesel-Diesel Blends. *Renew. Energy* **2017**, *107*, 440–447. [CrossRef]
20. Leevijit, T.; Prateepchaikul, G.; Maliwan, K.; Mompiboon, P.; Eiadtrong, S. Comparative Properties and Utilization of Un-Preheated Degummed/Esterified Mixed Crude Palm Oil-Diesel Blends in an Agricultural Engine. *Renew. Energy* **2017**, *101*, 82–89. [CrossRef]
21. Satputaley, S.S.; Zodpe, D.B.; Deshpande, N.V. Performance, Combustion and Emission Study on CI Engine Using Microalgae Oil and Microalgae Oil Methyl Esters. *J. Energy Inst.* **2017**, *90*, 513–521. [CrossRef]
22. Nirmala, N.; Dawn, S.S.; Harindra, C. Analysis of Performance and Emission Characteristics of Waste Cooking Oil and Chlorella Variabilis MK039712.1 Biodiesel Blends in a Single Cylinder, Four Strokes Diesel Engine. *Renew. Energy* **2020**, *147*, 284–292. [CrossRef]
23. Krishnamoorthi, M.; Malayalamurthi, R. Engine Characteristics Analysis of Chaulmoogra Oil Blends and Corrosion Analysis of Injector Nozzle Using Scanning Electron Microscopy/Energy Dispersive Spectroscopy. *Energy* **2018**, *165*, 1292–1319. [CrossRef]
24. Babu, D.; Thangarasu, V.; Ramanathan, A. Artificial Neural Network Approach on Forecasting Diesel Engine Characteristics Fuelled with Waste Frying Oil Biodiesel. *Appl. Energy* **2020**, *263*, 114612. [CrossRef]
25. Dharma, S.; Hassan, M.H.; Ong, H.C.; Sebayang, A.H.; Silitonga, A.S.; Kusumo, F.; Milano, J. Experimental Study and Prediction of the Performance and Exhaust Emissions of Mixed Jatropha Curcas-Ceiba Pentandra Biodiesel Blends in Diesel Engine Using Artificial Neural Networks. *J. Clean. Prod.* **2017**, *164*, 618–633. [CrossRef]
26. Banerjee, A.; Varshney, D.; Kumar, S.; Chaudhary, P.; Gupta, V.K. Biodiesel Production from Castor Oil: ANN Modeling and Kinetic Parameter Estimation. *Int. J. Ind. Chem.* **2017**, *8*, 253–262. [CrossRef]
27. Sandeep, K.B.; Naveen, K. Experimental investigation and artificial neural network modeling of performance and emission of a CI engine using orange peel oil-diesel blends. *Energy Sources Part A Recovery Util. Environ. Eff.* **2022**, *44*, 232–246.
28. Kolhe, A.V.; Malwe, P.D.; Wahile, G.S. Artificial intelligence for prediction of performance and emission parameters of CI engine using bio-fuel. *AIP Conf. Proc.* **2021**, *2369*, 020128.
29. Bahri, B.; Shahbakhti, M.; Aziz, A.A. Real-Time Modeling of Ringing in HCCI Engines Using Artificial Neural Networks. *Energy* **2017**, *125*, 509–518. [CrossRef]
30. Channapattana, S.V.; Pawar, A.A.; Kamble, P.G. Optimisation of Operating Parameters of DI-CI Engine Fueled with Second Generation Bio-Fuel and Development of ANN Based Prediction Model. *Appl. Energy* **2017**, *187*, 84–95. [CrossRef]
31. Niu, X.; Yang, C.; Wang, H.; Wang, Y. Investigation of ANN and SVM Based on Limited Samples for Performance and Emissions Prediction of a CRDI-Assisted Marine Diesel Engine. *Appl. Therm. Eng.* **2017**, *111*, 1353–1364. [CrossRef]
32. Esonye, C.; Onukwuli, O.D.; Ofoefule, A.U.; Ogah, E.O. Multi-Input Multi-Output (MIMO) ANN and Nelder-Mead's Simplex Based Modeling of Engine Performance and Combustion Emission Characteristics of Biodiesel-Diesel Blend in CI Diesel Engine. *Appl. Therm. Eng.* **2019**, *151*, 100–114. [CrossRef]
33. Çelebi, K.; Uludamar, E.; Tosun, E.; Yıldızhan, Ş.; Aydın, K.; Özcanlı, M. Experimental and Artificial Neural Network Approach of Noise and Vibration Characteristic of an Unmodified Diesel Engine Fuelled with Conventional Diesel, and Biodiesel Blends with Natural Gas Addition. *Fuel* **2017**, *197*, 159–173. [CrossRef]
34. Ramalingam, K.; Kandasamy, A.; Balasubramanian, D.; Palani, M.; Subramanian, T.; Varuvel, E.G.; Viswanathan, K. Forcasting of an ANN model for predicting behaviour of diesel engine energised by a combination of two low viscous biofuels. *Environ. Sci. Pollut. Res.* **2020**, *27*, 24702–24722. [CrossRef]
35. Thakur, A.K.; Mer, K.K.S.; Kaviti, A. An Artificial Neural Network Approach to Predict the Performance and Exhaust Emissions of a Gasoline Engine Using Ethanol–Gasoline Blended Fuels. *Biofuels* **2018**, *9*, 379–393. [CrossRef]
36. Ilangkumaran, M.; Sakthivel, G.; Nagarajan, G. Artificial Neural Network Approach to Predict the Engine Performance of Fish Oil Biodiesel with Diethyl Ether Using Back Propagation Algorithm. *Int. J. Ambient Energy* **2016**, *37*, 446–455. [CrossRef]
37. Soukht Saraee, H.; Taghavifar, H.; Jafarmadar, S. Experimental and Numerical Consideration of the Effect of CeO2 Nanoparticles on Diesel Engine Performance and Exhaust Emission with the Aid of Artificial Neural Network. *Appl. Therm. Eng.* **2017**, *113*, 663–672. [CrossRef]
38. LEE, T.; Singh, V.P.; Cho, K.H. Tensorflow and Keras Programming for Deep Learning. In *Deep Learning for Hydrometrology and Envinormental Scienece*; Springer: Berlin/Heidelberg, Germany, 2021; pp. 151–162. [CrossRef]
39. Nurdiyana Wan Mansor, W.; Abdullah, S.; Ashraf Razali, N.; Albani, A.; Ramli, A.; Olsen, D. Prediction of Emissions of a Dual Fuel Engine with Artificial Neural Network (ANN). In Proceedings of the 2019 Theory and Technique International Aerosol Conference and Malaysia Air Quality Annual Symposium, Balik Pulau Hotel, Malacca, Malaysia, 7–10 August 2019; IOP Conference Series: Earth and Environmental Science; Institute of Physics Publishing: Bristol, UK, 2019; Volume 373.
40. Javed, S.; Satyanarayana Murthy, Y.V.V.; Baig, R.U.; Prasada Rao, D. Development of ANN Model for Prediction of Performance and Emission Characteristics of Hydrogen Dual Fueled Diesel Engine with Jatropha Methyl Ester. Biodiesel Blends. *J. Nat. Gas Sci. Eng.* **2015**, *26*, 549–557. [CrossRef]

41. Rajak, U.; Nashine, P.; Verma, T.N. Effect of Spirulina Microalgae Biodiesel Enriched with Diesel Fuel on Performance and Emission Characteristics of CI Engine. *Fuel* **2020**, *268*, 117305. [CrossRef]
42. Rajak, U.; Verma, T.N. Spirulina Microalgae Biodiesel—A Novel Renewable Alternative Energy Source for Compression Ignition Engine. *J. Clean. Prod.* **2018**, *201*, 343–357. [CrossRef]
43. Rahman, M.A.; Aziz, M.A.; Ruhul, A.M.; Rashid, M.M. Biodiesel Production Process Optimization from Spirulina Maxima Microalgae and Performance Investigation in a Diesel Engine. *J. Mech. Sci. Technol.* **2017**, *31*, 3025–3033. [CrossRef]
44. Nautiyal, P.; Subramanian, K.A.; Dastidar, M.G.; Kumar, A. Experimental Assessment of Performance, Combustion and Emissions of a Compression Ignition Engine Fuelled with Spirulina Platensis Biodiesel. *Energy* **2020**, *193*, 116861. [CrossRef]
45. Arunkumar, M.; Kannan, M.; Murali, G. Experimental Studies on Engine Performance and Emission Characteristics Using Castor Biodiesel as Fuel in CI Engine. *Renew. Energy* **2019**, *131*, 737–744. [CrossRef]
46. Mohamed, M.; Tan, C.-K.; Fouda, A.; Gad, M.S.; Abu-Elyazeed, O.; Hashem, A.-F. Diesel Engine Performance Emissions and Combustion Characteristics of Biodiesel and Its Blends Derived from Catalytic Pyrolysis of Waste Cooking Oil. *Energies* **2020**, *13*, 5708. [CrossRef]